

RANSEs Simulation of the Flow past a Marine Propeller under Design and Off-design Conditions

Lucia Sileo, Aldo Bonfiglioli and Vinicio Magi

*Department of Environmental Engineering and Physics, University of Basilicata
Viale dell'Ateneo Lucano 10, 85100 Potenza, Italy.*

Email: *lsileo@unibas.it*

ABSTRACT

In the present work the results of a preliminary computational fluid dynamics (CFD) simulation of the flow past a marine propeller are presented. The principal aim of the study is to verify the ability of a CFD method, solving the Reynolds-Averaged Navier-Stokes Equations (RANSEs), to predict the performances of a marine propeller. The complexity in the mesh generation is one of the main obstacles for CFD. Following an hybrid mesh generation approach, prismatic cells have been generated in the boundary layer, where viscous phenomena are dominant, and tetrahedral cells in the remaining regions. A parallel RANS solver has been used, employing a cell-centered, finite-volume method that allows the use of computational cells of arbitrary polyhedral shape. Boundary conditions were given to simulate the flow past a rotating propeller in open water conditions. The equations have been written in a moving reference frame fixed on the propeller blades. The steady-rotating reference frame source terms, i.e., the centrifugal and Coriolis force terms, therefore, are added to the RANS equations derived in the inertial frame. The $k-\omega$ model has been employed for turbulence closure. Different values of advance ratios are considered, at design and off-design conditions. Computational results have been obtained for all the four-quadrant operational conditions: forward, backing, crashback and crashahead, considering also non-positif values for the advance ratio J . The thrust and torque coefficients, k_T and k_Q , have been selected as global quantities and compared with available experimental data. Pressure and velocity distributions and turbulent quantities were also used to analyze the computed flow field. The results show a good qualitative agreement with the experimental data. Important issues need to be addressed like an extensively improvement in the mesh generation techniques and in turbulence modeling.

1 INTRODUCTION

The flow past a marine propeller is one of the most challenging problems in the computational fluid dynamics (CFD). In the last few years, remarkable improvements in numerical modeling of viscous flows around marine propellers have been obtained.

Various numerical simulation approaches (boundary elements, panel methods, etc.) for studying marine propeller geometries have been used for decades, but only recently, due to the rapid advances in computer power and in the parallelization capabilities, different CFD methods, and in particular Reynolds Averaged Navier-Stokes (RANS) equation solvers, are increasingly applied to simulate the full three-dimensional viscous and turbulent flow for various propeller geometries [1]–[7]. Since structured grids have been used in most cases, computational results have been limited to steady flow in open water conditions, in the case of uniform inflow and non-cavitating conditions. The use of unstructured mesh is suitable for improvement of accuracy and for future extension to unsteady and cavitating flows, and for investigation of the hull-propeller interaction [8]–[10].

Also LES approaches start to be used to analyze marine propeller flows [11], but CFD methods solving the RANSEs are still recognized as the most appealing approach for marine propeller geometries, primarily because the computational time and resources are reasonably practical compared to LES and DNS.

Despite the great advancement in the CFD technologies and feasibilities of the approaches for marine propeller flows, some issues need to be addressed for more practicable procedures. The complexity in the mesh generation and turbulence modeling are the main obstacles. In fact a marine propeller is a very complex geometry, with variable section profiles, chord lengths and pitch angles, and in operational conditions it induces rotating flow and entails tip vortex. For turbu-

lence closure, however, the use of a $k-\omega$ model [12] is deemed sufficient for engineering applications, being the mesh quality more critical than the turbulence anisotropy prediction [8].

1.1 Propeller Model

In the present work a propeller designed to operate on a Remotely Operated Vehicle (ROV) is investigated. Unmanned Underwater Vehicles (UUV) are normally actuated and dynamically positioned by bladed thrusters, as many other marine vehicles, like submarines, submersibles and ships.

An ROV is not designed to move at high speed in water, instead it works especially at very low speed, in the hovering and in station-keeping, for samples or images gathering, then it operates overall at heavy load operational conditions, corresponding to very low values of the advance ratio coefficient. On the other hand, propellers are usually not designed for these operational conditions. In these regimes, nonlinearities related to thrusters dynamics become very important and they can influence the overall system behavior and make difficult the accurate control of the low-speed trajectory of an underwater vehicle [14]. In fact the problem of the thruster dynamics and its influence on the behavior of dynamically positioned marine vehicles still remains to be solved and in the last few years it is focusing the attention of many studies [14]–[16].

A better understanding of propeller hydrodynamics, including an accurate description of the three-dimensional rotational flow and a detailed estimation of the pressure field for the investigation of the cavitation inception can be very important for many scientific and practical purposes and it can be provided both through experimental and numerical techniques.

The occurrence of strong vortical structures, turbulent fluctuations and marked velocity gradients puts very strict requirements on the choice of measurements techniques. The development of non-intrusive techniques, such as Laser Doppler Velocimetry (LDV) and Particle Image Velocimetry (PIV), allows suitable experimental investigations of such complex fluid dynamic phenomena, and detailed experiments have been recently performed [17]–[19]. Unfortunately for heavy load and off-design operations, only limited information is available and detailed flow measurements are lacking or they are extremely difficult and expensive to perform. This is why accurate numerical simulations could be even more useful, but it is necessary to improve their ability to accurately predict the complex involved phenomena.

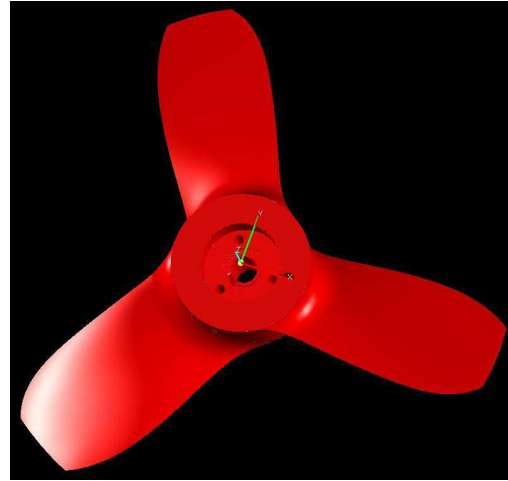


Figure 1: *Propeller geometry.*

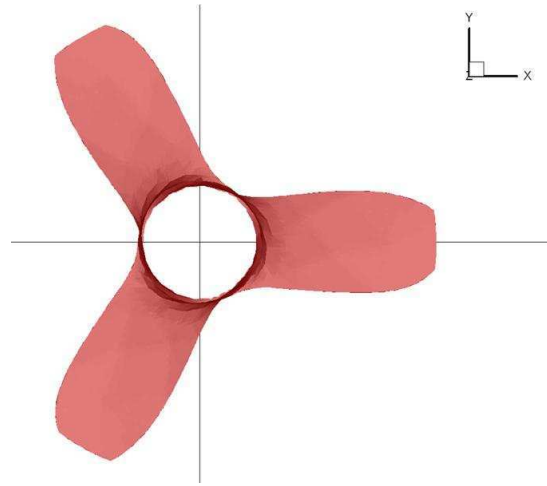


Figure 2: *Geometry simplifications.*

2 NUMERICAL IMPLEMENTATION

2.1 Model Geometry

The present simulations are performed on a small three-bladed propeller with the diameter $D = 0.16m$. It has been mounted on Romeo, an ROV designed by the RobotLab [13] in Genoa, Italy. The propeller geometry is shown in Fig. 1.

The preliminary phase to this work has been conducted by the RobotLab where the CAD drawing has been obtained directly from the propeller itself. Then the pre-processing phase is followed at the computational laboratory of the University of Basilicata. The pre-processor Pro-Surface of Star-Cd software (by Cd-Adapco) was used for importing the geometry file.

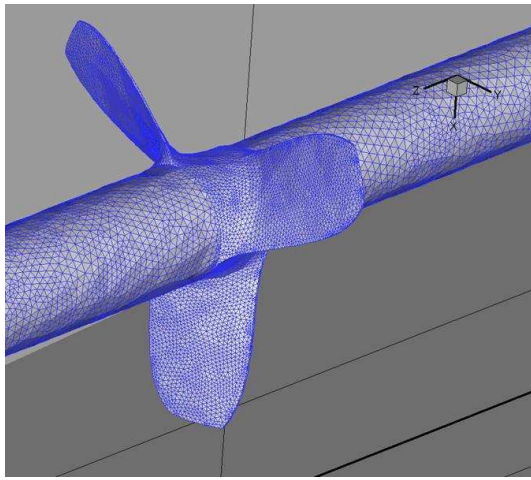


Figure 3: *Mesh distribution on the surface of the blades and infinite hub.*

Then further corrections and simplifications have been necessary as it is shown in Fig. 2.

2.2 Computational Domain

After simplifications, the blades have been simply mounted on an infinitely long cylinder, which serves as the hub and shaft, to avoid the stagnation point on the hub close to the propeller, as illustrated in Fig. 3. The computational domain has been identified with a cylinder surrounding the propeller and aligned with the hub axis. If D is the propeller diameter, the inlet is $4D$ upstream, the outflow $6D$ downstream, the diameter of the lateral cylindrical boundary is $5D$. Uniform inflow is aligned with the z-axis of the coordinate system, whose origin is placed on the solid surface of the propeller and located on the central axis of the domain, as shown in Fig. 4.

2.3 Mesh Generation

The Pro-Star Auto-Meshing was used for the mesh generation. The surfaces on the hub/shaft and blades have been triangulated and optimized for tetrahedral meshing. Ten layers of prismatic cells have been attached to the blades and hub surface, and the remaining domain has been filled with tetrahedral cells. The final mesh is composed of about 2 million cells. The height of the first cell adjacent to the solid surface is approximately $0.0001D$, which is 1 to 30 in terms of y^+ for all surfaces.

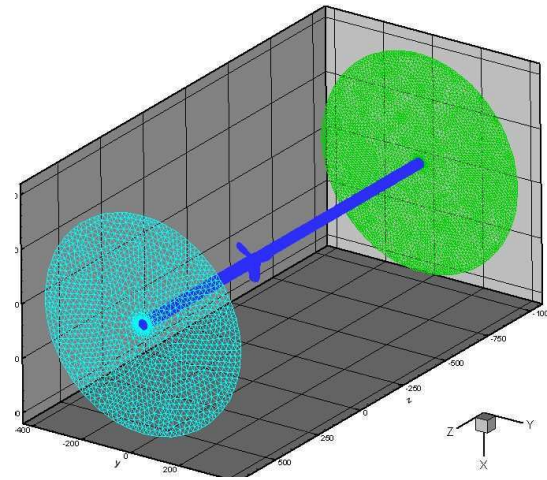


Figure 4: *The computational domain: inlet and exit boundaries.*

2.4 Boundary Conditions

Boundary conditions were set to simulate the flow around a rotating propeller in open water: on the inlet boundary, velocity components of uniform stream with the given inflow speed were imposed; on the exit boundary, the static pressure was set to constant while the other variables were extrapolated; on the outer boundary, the symmetry boundary condition was imposed; on the blade and hub surface, the no-slip condition was imposed.

The boundary conditions are set to reproduce the flow past a marine propeller in an infinite domain, then they do not reproduce properly the experimental conditions in the water tunnel, leading to an over-prediction of the non-dimensional K_T and K_Q . In fact it has been seen that the water tunnel results are generally lower than the respective tow-tank values [11].

2.5 Numerical Method

The commercial solver Comet [20], developed by ICCM, is applied to calculate the rotating propeller flow. The code run in parallel mode on 6 bi-processor nodes on a Linux Beowulf Cluster HP-IA32 with 40 bi-processor node ProLiant DL360. The space parallelization has been implemented in Comet using MPI message passing libraries.

The present computations are conducted on a rotating frame which is fixed on the propeller blades. In fact when a domain rotates at a constant angular velocity, the analysis can be simplified if the problem is analyzed in a coordinate system which rotates together

with this domain. The setting of a rotating domain makes no influence in Comet on the specification of boundary velocities - they are given in the same way as in the case when the domain is stationary. The steady-rotating reference frame source terms, i.e., the centrifugal and Coriolis force terms, therefore, are added to the RANS equations derived in the inertial frame. The limited experimental data for validation and the initial (exploratory) nature of the present study have motivated the selection of the discretization scheme. A compromise between the robustness of the upwind differencing and the accuracy of the other higher-order schemes has been selected. As a steady solution was expected, it has been considered advisable to use the upwind scheme first for a new problem, and re-start the computation with a higher value of the blending factor for the transient calculations.

The so-called pseudo-transient procedure has been used for achieving stability of steady-state calculations. It retains the transient rate of change term, takes a relatively large time step and does only one iteration per time step. It is therefore not time accurate, but that is not important since the steady-state is sought. This procedure is particularly useful in calculating flows where it is difficult to get a reasonable initial dependent variable fields, e.g. in situations when the mass flow rate through the solution domain is not known in advance. The first-order Euler implicit approximation method is applied to the pseudo-time derivatives.

After a steady solution has been computed, to be sure that the flow is really steady, an unsteady simulation has been carried out with the existing steady flow field as the initial condition. A quasi-second-order central discretization scheme has been used for the spatial differencing of the convective terms with a blending factor equal to 0.9, and a second-order central differencing for the viscous terms.

In order to calculate the pressure field and to couple it properly to the velocity field, a pressure-correction method of SIMPLE-type segregated algorithm adapted to unstructured grid was used. The resulting system of algebraic equations was solved by a Incomplete Cholesky Preconditioned Conjugate Gradient solver.

2.6 Turbulence Model

The $k-\omega$ model has been used for turbulence closure, it is reckoned to perform very well close to walls in boundary layer flows, particularly under strong adverse pressure gradients.

This model is able to resolve the viscous sub-layer, eliminating the need to use wall functions, but in Comet it is possible to use wall functions for computa-

tional efficiency. It depends from the resolution of the mesh: if the first grid point is in the viscous sub-layer ($y^+ < 2.5$) the low-Reynolds formulation of the models is activated and the equations are integrated from the boundary conditions on the wall. Otherwise, when the near-wall cell is located in the fully developed part of the boundary layer, a high-Reynolds implementation is used with adequate wall functions. This is very useful when the grid is not optimized, like in the present case, because of the extremely complexity of the geometry. The code is able to automatically switch from a high-Reynolds formulation to a low-Reynolds formulation in terms of the resolution of the mesh.

3 RESULTS AND ANALYSIS

To analyze the computational results, global and local quantities are selected. The thrust and torque coefficients, k_T and k_Q , are selected as the global quantities of interest:

$$k_T = \frac{T}{\rho n |n| D^4}; \quad k_Q = \frac{Q}{\rho n |n| D^5}; \quad J = \frac{U}{n D} \quad (1)$$

where U is the advance (or freestream) velocity, n is the propeller angular velocity, D the propeller diameter, T the thrust and Q the torque, while J is defined as the advance ratio.

Conditions related to $n = 1500\text{rpm}$ and different values of the advance ratio J were numerically simulated but validation against the experimental data is possible only for global quantities and in forward conditions. First the pseudo-transient simulations of the four-quadrant operational conditions are carried out: target residuals were set at 10^{-6} and the maximum iteration number was 2000, sufficient for the residuals to fall below the target. The time step was set as 0.04s , corresponding to 360 degrees of propeller rotation. Typical results for the four-quadrant conditions are shown in Fig. 5.

The comparison with the experimental data for both thrust and torque coefficients is illustrated in Fig. 6. The results agree reasonably well with the data [21], especially in considerations of the difference in boundaries between the CFD and the experiments (i.e., water tunnel for the experiments vs. the infinite assumption for the calculations), and the modifications of the geometry (i.e. infinite hub). Furthermore experimental uncertainty has not been provided from the RobotLab. The predicted thrust coefficient shows a good agreement with the experimental data, while the torque coefficient is over-predicted. This discrepancy is just noted in the literature [3, 4, 6, 7, 8, 10] and usually increases with increasing propeller load [4, 7, 8]. The possible causes are in the grid quality and in the turbu-

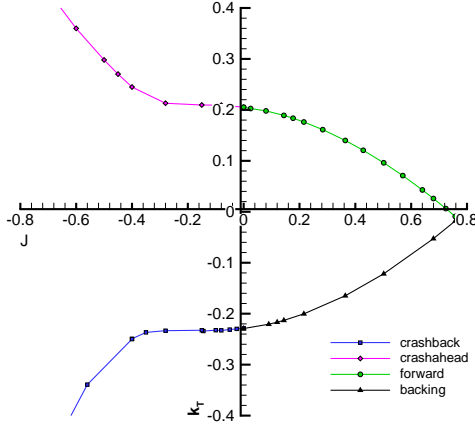


Figure 5: Thrust coefficient versus advance ratio for all four-quadrant operational conditions.

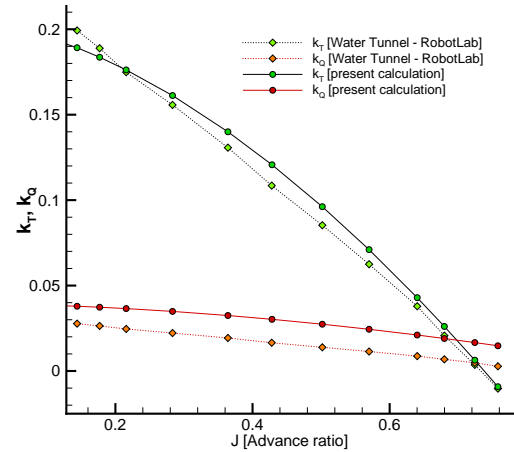


Figure 6: Thrust and Torque coefficients versus advance ratio: comparison with experimental data.

lence modeling. In fact the torque coefficient is more dependent of the grid quality at the edge of the propeller [6], and it is strongly related to the deficiencies of the turbulent model in predicting the tangential velocity field. Similar poor predictions have been experimentally proved and documented also for impeller-like flow simulations with other RANSEs commercial codes [22].

The subsequent transient simulations were carried out with a small time step corresponding to 6 degrees of propeller rotation. The target residuals were set at 10^{-4} and the maximum iteration number per time step was 100.

In the following, the results for $J = 0.1441$ are illustrated. In Fig. 7 the non-dimensional thrust K_T and torque K_Q are plotted as they change during the computation. The horizontal axe shows time elapsed since the beginning of the transient calculation in propeller revolutions. Both thrust and torque approach a steady state. Compared to the pseudo-transient results, there is an improvement in the torque prediction, which proves to be more sensible to the low accuracy of the upwind differential scheme applied for pseudo-transient calculation, as it is shown in Tab. 1.

It is not possible to make any type of comparison with experimental data for pressure, velocity and turbulence distributions, hence in the next figures only numerical results are showed for $J = 0.1441$, as obtained in transient calculation.

Figs. 8 and 9 show the streamlines and the contour plots respectively of the axial-velocity, normalized by the free-stream velocity, and of the pressure coefficient

Table 1: Comparison of the thrust and torque coefficients as obtained in the pseudo-transient and in transient calculations respectively and in water tunnel experiments [21], for $J = 0.1441$.

	K_T	K_Q
pseudo-transient	0.1892	0.03790
transient	0.1868	0.03328
water tunnel	0.1993	0.02772

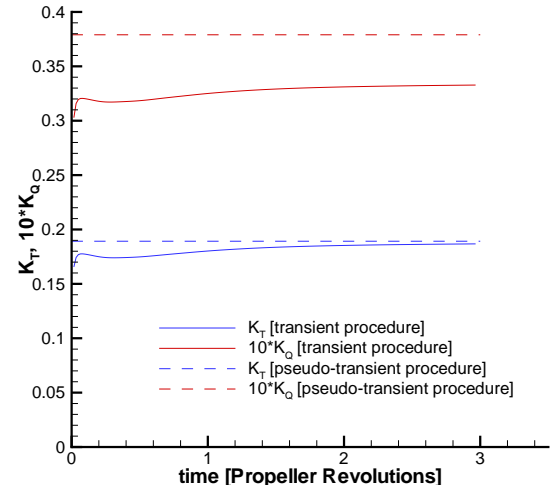


Figure 7: K_T and K_Q plot during transient computation.

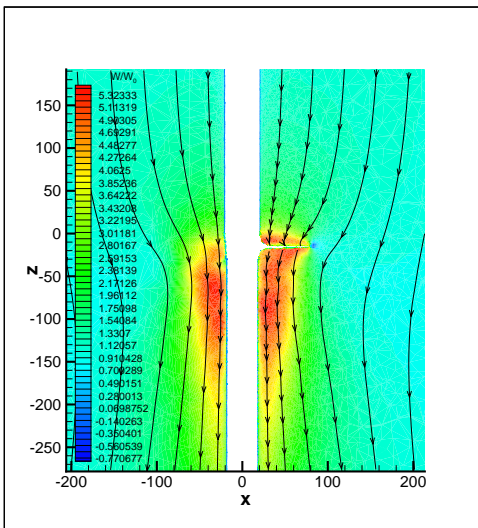


Figure 8: Streamlines and contour plot of the axial-velocity normalized by the free-stream velocity, in a longitudinal axial plane.

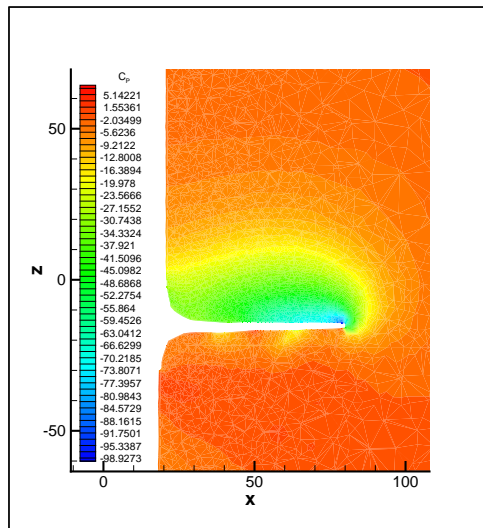


Figure 9: Contour plot of the pressure coefficient, in a longitudinal axial plane.

in a longitudinal axial plane. It is possible to note how the flow is accelerated through the propeller disc, the distortion of the streamlines and the suction and the pressure side on the blade. In correspondence of the tip of the blade a recirculating zone is visible where the axial velocity is opposed to the main flow, and a very low value of the pressure coefficient.

In Fig. 10 the turbulent viscosity, the root-mean-square of turbulent velocity fluctuation ($q = \sqrt{2k}$, where k is the turbulent kinetic energy) and the axial-velocity 3-D contour plots are showed in a cross plane corresponding to the middle section of the propeller.

In Fig. 11 the axial-velocity contour plots are illustrated on the same plane, respectively with absolute and relative streamlines, that is obtained with absolute and relative velocities. In Fig. 12 are plotted the relative streamlines and the contours plots respectively of the turbulence viscosity and of the tangential relative velocity, in a plane $x = 0.7R$, where R is the radius of the propeller.

4 CONCLUSIONS

In this report the first preparatory approach to the study of the flow past a marine propeller is described. A parallel RANSe solver employing a cell-centered, finite-volume method that allows the use of computational cells of arbitrary polyhedral shape, has been used to predict the performances of a marine propeller. An hybrid mesh generation approach has been used to cope with the complexity of the problem geometry,

i.e., prismatic cells have been generated in the boundary layer, where viscous phenomena are dominant, and tetrahedral cells in the remaining regions. The computational efficiency has been pursued and motivated by the limited experimental data for validation and the initial (exploratory) nature of the present study. As a steady solution was expected, a pseudo-transient calculation with an upwind differential scheme was used first for a new problem, then a transient calculation was re-started with a higher value of the blending factor. The numerical results are, as a whole, acceptable and their quality is comparable with the numerical predictions obtained with different approaches and/or solvers using a considerable greater amount of computational resources.

Important issues need to be addressed like the refinement in the tip vortex region and an extensively improvement in the mesh generation technique, that has been the main obstacle. The results and the experience acquired during this work suggest first of all the necessity of a grid refinement and preferably a variation of the computational domain, eliminating the infinite hub and reducing the extent of the computational domain. The turbulence modeling is also an important outstanding issue: eddy-viscosity models, based on the assumption of local isotropic turbulence, clearly show to be inadequate in describing a flow field largely anisotropic, then maybe a more complex (anisotropic) turbulence model is needed. The study of a new propeller geometry, with more detailed experimental data, represents the obvious continuation of the present work and the aim of our future activity.

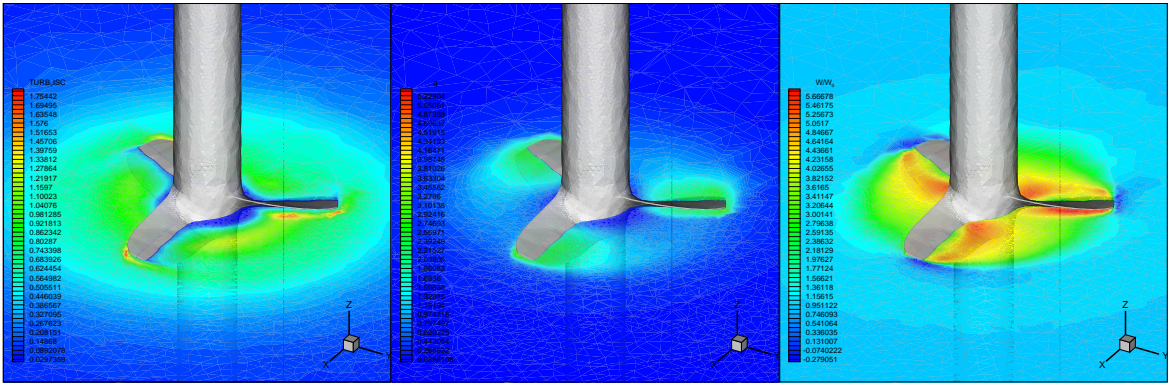


Figure 10: 3-D contour plots of the: (left) Turbulent viscosity; (center) root-mean-square of turbulent velocity fluctuation ($q = \sqrt{2k}$); (right) axial-velocity.

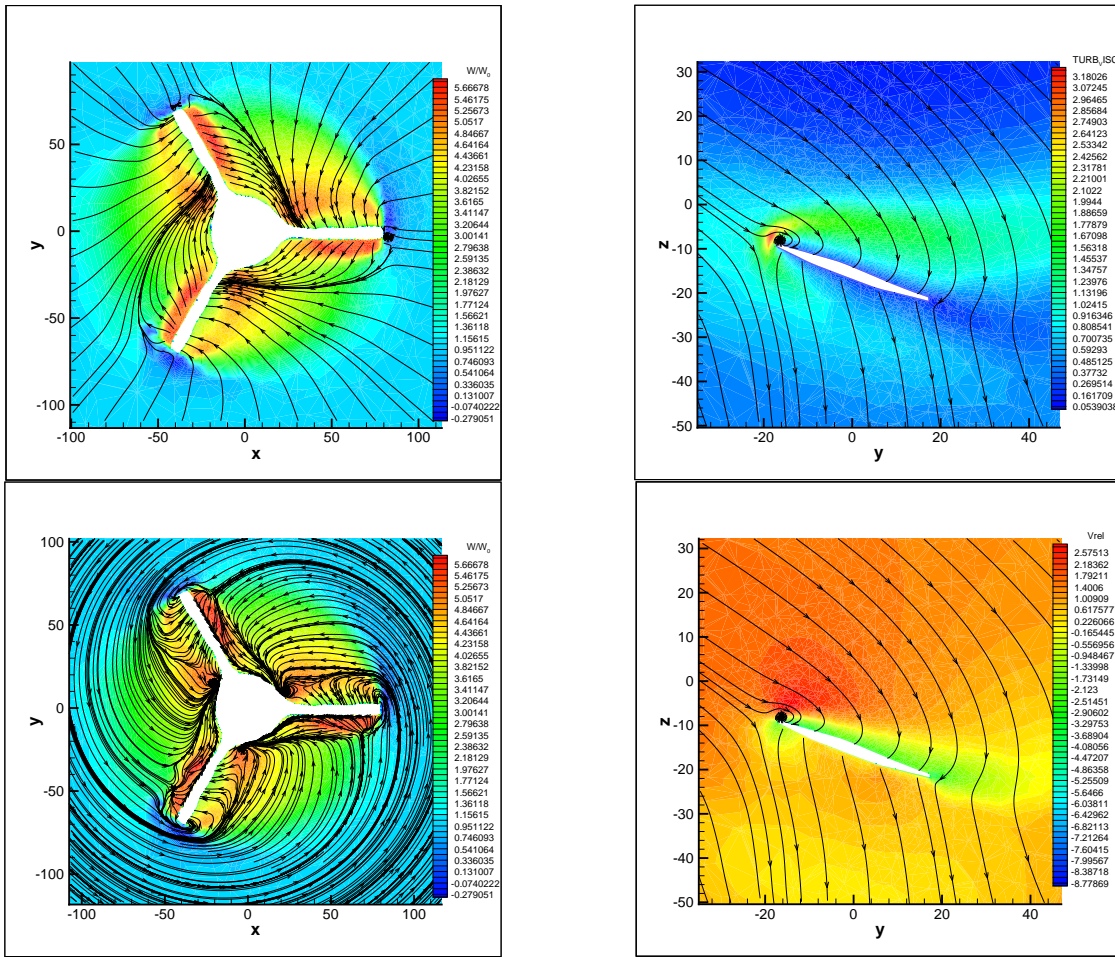


Figure 11: Axial-velocity contour plots on a cross plane corresponding to the section plane of the propeller, respectively with: (upper) absolute; and (lower) relative streamlines.

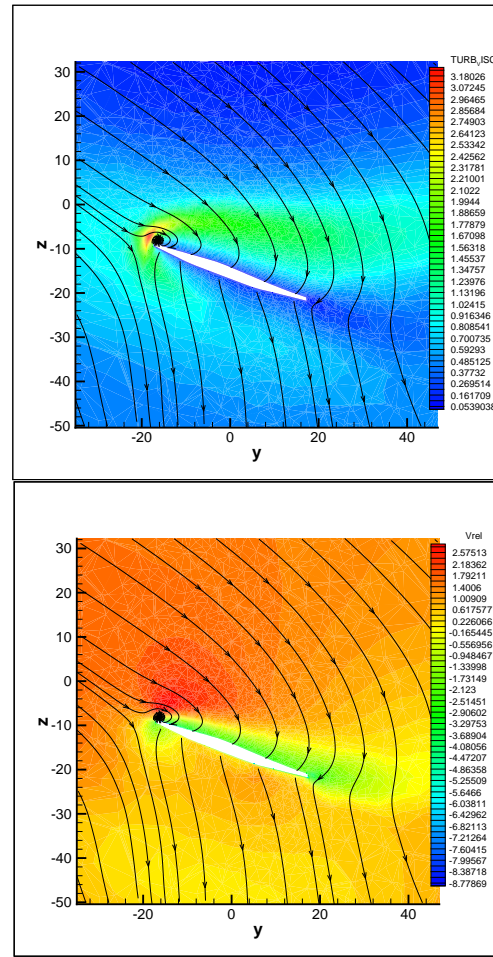


Figure 12: Relative streamlines and contour plots respectively of the: (upper) turbulence viscosity; and (lower) tangential relative velocity, in an plane $x = 0.7R$, where R is the radius of the propeller.

REFERENCES

- [1] M. Abdel-Maksoud, F. Menter and H. Wuttke. Viscous flow simulations for conventional and high-skew marine propellers. *Ship Technology Research*, 45:64–71, 1998.
- [2] M. Abdel-Maksoud and H.-J. Heinke. Scale Effects on Ducted Propellers. Twenty-fourth ONR Symposium on Naval Hydrodynamics, Fukuoka, Japan, 744–759, 2002.
- [3] B. Chen and F. Stern. Computational Fluid Dynamics of Four-Quadrant Marine-Propulsor Flow. *Journal of Ship Research*, 43(4): 212–228, 1999.
- [4] C.T. Hsiao and L.L. Pauley. Numerical Computation of Tip Vortex Flow Generated by a Marine Propeller. *ASME Journal Fluids Engineering*, 121: 638–645, 1998.
- [5] K.-J. Oh and S.-H. Kang. Numerical calculation of the viscous flow around a propeller shaft configuration. *International Journal of Numerical methods in Fluids*, 21(1):1–13, 1995.
- [6] A. Sánchez-Caja, P. Rautanhiemo and T. Siikonen. Simulation of Incompressible Viscous Flow Around a Ducted Propeller Using a RANS Equation Solver. 23rd Symposium on Naval Hydrodynamics, Val de Reuil, France, 527–539, 2000.
- [7] M. Stanier. The Application of ‘RANS’ Code to Investigate Propeller Scale Effects. 22nd Symposium on Naval Hydrodynamics, 222–238, 1999.
- [8] S.H. Rhee and S. Joshi. CFD Validation For A Marine Propeller Using An Unstructured Mesh Based Rans Method. *Proceedings of FEDSM’03, 4th ASME-JSME Joint Fluids Engineering*, Summer Conference, Honolulu, Hawaii, USA, 2003.
- [9] S.H. Rhee, E. Koutsavdis. Two-dimensional simulation of unsteady marine propulsor blade flow using dynamic meshing techniques. *Computers Fluids* 34, 1152–1172, 2005.
- [10] T. Watanabe, T. Kawamura, Y. Takekoshi, M. Maeda and S.H. Rhee. Simulation of Steady and Unsteady Cavitation on a Marine Propeller Using a RANS CFD Code. 5th Int. Symposium on Cavitation, paper GS-12-004, Osaka (Japan), November 2003.
- [11] M. Vysohlid and M. Mahesh. Large Eddy Simulation of propeller Crashback. Aerospace Engineering & Mechanics , University of Minnesota, RTO-MP-AVT-123, 2004.
- [12] D.C. Wilcox. Turbulence Modeling for CFD, 2nd Ed., DCW Industries, Inc., La Canada, Ca, 1998.
- [13] RobotLab, Marine Robotics Department at Istituto per l’Automazione Navale (IAN), National Research Council, Genoa, Italy. Private Communications.
- [14] D.R. Yoerger, Cooke J.G. and J.-J.E. Slotine. The Influence of Thruster Dynamics on Underwater Vehicle Behavior and Their Incorporation Into Control System Design. *IEEE Journal of Oceanic Engineering*, 15(3):167–178, 1990.
- [15] R. Bachmayer, L.L. Whitcomb and M.A. Grosenaugh. An Accurate Four-Quadrant Nonlinear Dynamical Model for Marine Thrusters: Theory and Experimenat Validation. *IEEE Journal of Ocean Engineering*, 25(1): 146–159, 2000.
- [16] L.L. Withcomb and D.R. Yoerger. Development, Comparison, and Preliminary Experimental Validation of Nonlinear Dynamic Thruster Models. *IEEE Journal of Oceanic Engineering*, 24(4):481–494, 1999.
- [17] C.J. Cheskas and S.D. Jessup. Experimental Characterization of Propeller Tip Flow. *Proc., 22nd Symposium on Naval Hydrodynamics*, Washington, DC, 1998.
- [18] A. Cotroni, F. Di Felice, G.P. Romano and M. Elefante. Investigation of the Near wake of a Propeller Using Particle Image Velocimetry *Experiments in Fluids* [Suppl.], S227–S236, 2000.
- [19] A. Stella, G. Guj, F. Di Felice and M. Elefante. Propeller Wake Evolution Analysis by LDV. *Proc., 22nd Symposium on Naval Hydrodynamics*, Washington, DC, 1998.
- [20] CoMET, Continuum Mechanics Engineering Tool, by ICCM, Institute of Computational Continuum Mechanics GmbH, CD adapco Group. <http://www.iccm.de>.
- [21] G. Bruzzone and E. Spirandelli. Caratterizzazione del modulo pro-pulsore del veicolo Romeo tramite prove sperimentalni in Tunnel di Cavitazione TR 248, 1996.
- [22] M. Li, G. White, D. Wilkinson and K.J. Roberts. LDA Measurements and CFD Modelling of a Stirred Vessel with a Retreat Cyrve Impeller. *Ind. Eng. Chem. Res.*, 43(6534–6547), 2004.